Supplemental material

Supplemental figure legends

Figure S1 Expression of *AHL* gene family members in diploid (L*er* × Col) and triploid (L*er* × *osd1*) seeds. *AHLs* from clade B are labelled with (I), and *AHLs* from clade A are labelled with (II).

Figure S2 Localization and expression of ADM and SUVH2/9. Fusion constructs with GFP (A-C) or N- or C-terminal domains of YFP (nYFP or cYFP) (D-G) were expressed in *N. benthamiana* leaves. Water-mounted sections of leaf tissue were examined by confocal microscopy. Scale bars, 5µm. (A) SUVH9-GFP, (B) ADM-GFP, (C) AHL10-GFP, (D) ADM-cEYFP and nEYFP-SUVH9, (E) ADM-cEYFP and AHL10-nEYFP, (F) AHL10-cEYFP and nEYFP-SUVH9, (G) AHL10-nEYFP and AHL10-cEYFP. Scale bars, 10 µm. (H) Quantitative RT-PCR analysis of *SUVH2* and *SUVH9* expression in seeds derived from indicated crosses at 6 DAP. Data were normalized to *PP2A*.

Figure S3 Bar chart representing z-scored normalized H3K27me3 values on maternal and paternal alleles of *PHE1*, *ADM*, *SUVH9*, and *AHL10*.

Figure S4 Triploid seed abortion is rescued by *suvh9* and *ahl10*. (A) Percentage of non-collapsed (gray bars) and germinated seeds (black bars) of indicated genotypes. Numbers on top of bars correspond to number of analyzed seeds. (B and C) Pictures of seedlings at 7 days after germination of indicated genotypes. Scale bars, 1 cm. (D) Percentage of non-collapsed seeds of indicated genotypes. Numbers on top of bars correspond to number of analyzed seeds. (E and F) Complementation of *osd1 ahl10* and

osd1 suvh9 using constructs expressing *AHL10* and *SUVH9* under control of the *UBIQUITIN* (*UBQ*) and (*PHE1*) promoters. Col plants were pollinated with pollen of *osd1 ahl10* or *osd1 suvh9* with or without the indicated complementation construct. Col plants pollinated with *osd1* pollen served as a control. Independent transgenic lines are numbered. Numbers on top of bars correspond to number of analyzed seeds.

Figure S5 (A) Metagene plots showing z-score normalized H3K9me2 for all five chromosomes in the endosperm of seeds derived from crosses Col × Col (Col), Col × *osd1* (3x Col), Col × 2x *adm* (2x *adm*), Col × *osd1 adm* (3x *adm*), Col × 2x *suvh2 suvh9* (2x *suvh2 suvh9*), Col × 4x *suvh2 suvh9* (3x *suvh2 suvh9*), Col × 2x *ahl10* (2x *ahl10*), Col × 4x *ahl10* (3x *ahl10*). (B) Metagene plots showing z-score normalized H3K9me2 at TEs in the genotypes specified in A. (C) Metagene plots showing CHH DNA methylation (#C/(#C+#T) at TEs in the endosperm of Col, 3x Col, and 3x *adm*.

Figure S6 (A) Box plots showing median values of z-score normalized H3K9me2 in predicted matrix attachment regions (MAR), regions excluding MARs (Not MAR), predicted MARs overlapping transposable elements (MAR (TE)), and transposable elements (TE) in the endosperm of seeds derived from crosses Col × Col (Col), Col × *osd1* (3x Col), Col × *osd1 adm* (3x *adm*), Col × 4x *suvh2 suvh9* (3x *suvh2 suvh9*), Col × 4x *ahl10* (3x *ahl10*). The difference between Col and 3x Col, 3x Col and 3x *adm,* 3x Col and 3x *suvh2 suvh9,* 3x Col and 3x *ahl10* in MARs, MAR(TE)s, and TEs are significant (Kolmogorov–Smirnov test, $p<10E^{-15}$). (B) Boxplot showing z-score normalized H3K9me2 in predicted matrix attachment regions (MAR), regions excluding MARs (Not MAR), predicted MARs overlapping transposable elements (MAR (TE)), and transposable

elements (TE) in the indicated genotypes. Boxes show medians and the interquartile range, error bars show the full range excluding outliers.

Figure S7 (A) Log2 fold expression change of transposable elements gaining H3K9me2 in 3x Col ($p<0.05$) with detectable transcript levels in 2x Col, 3x Col, or 3x *adm* seeds. (B) Log2 fold expression change of genes flanking TEs significantly gaining H3K9me2 in 3x Col ($p<0.05$) in 2x Col and 3x Col seeds. All genes were used as control. The difference is significant (Kolmogorov–Smirnov test$p<0.01$). (C) Log2 fold expression change of genes with increased expression in 3x Col and genes flanking TEs significantly gaining H3K9me2 in 3x Col ($p<0.05$) in 3x Col and 3x *adm* seeds. The difference is significant (Kolmogorov–Smirnov test, $p <0.05$).

Figure S8 H3K9me2 methylation profiles of *HDG10*, *AT1G35183*, *PEG4*, *PEG7*, and *PEG9* in the endosperm. The profiles are derived from endosperm of the following genotypes: Col (brown), 3x Col (cyan), 3x *adm* (blue), 3x *suvh2;9* (red), 3x *ahl10* (green). Regions with changes in H3K9me2 are marked by red dashed rectangles. Black horizontal bar: coding region of genes; blue horizontal bar: transposable element.

Figure S9 (A) Metagene plots showing z-score normalized H3K9me2 levels in 4 DAP endosperm derived from crosses Col × *osd1* (3x Col), Col × *osd1 adm* (3x *adm*), and Col × Col (2x Col) seeds. TEs belonging to RC/helitron, DNA MuDR, and DNA/HAT families that gained H3K9me2 in triploid seeds are shown. (B) Metagene plots showing DNA methylation (#C/(#C+#T) in each sequence context in samples specified in A. (C)

Metagene plots showing CHH methylation of TEs defined above in 6 DAP endosperm of3x Col and 2x Col seeds.

Figure S10 Log2 fold change of expression of *MORCs* in 3x Col *versus* Col.

Jiang_Fig S1

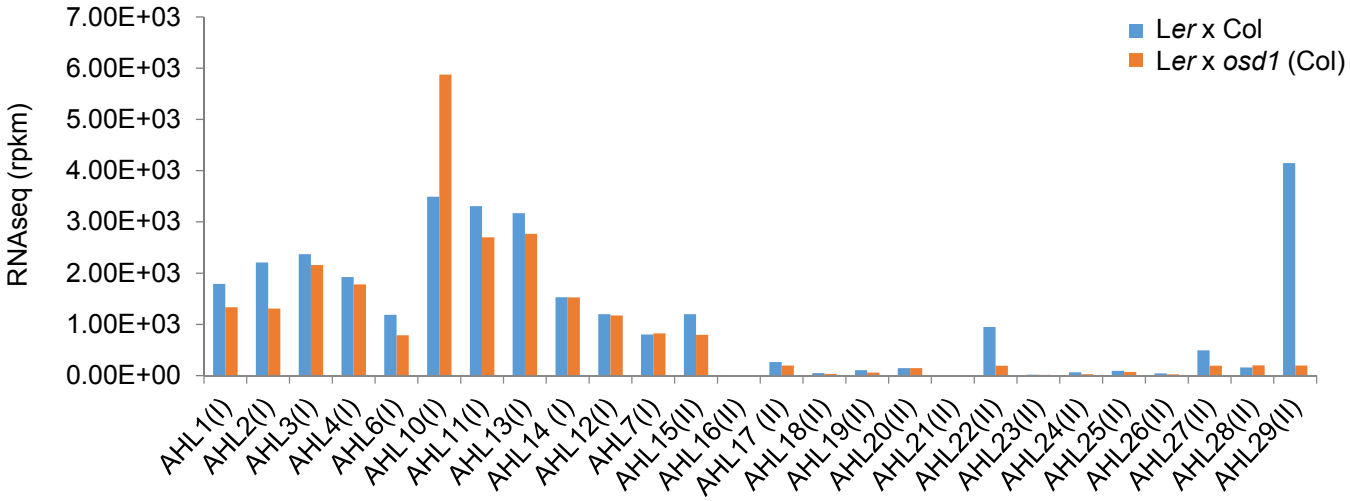
RNAseq (rpkm)
7.00E+03
6.00E+03
5.00E+03
4.00E+03
3.00E+03
2.00E+03
1.00E+03
0.00E+00
Ler x Col
Ler x osd1 (Col)
AHL1(I)
AHL2(I)
AHL3(I)
AHL4(I)
AHL6(I)
AHL10(I)
AHL11(I)
AHL13(I)
AHL 14 (I)
AHL12(I)
AHL7(I)
AHL15(II)
AHL16(II)
AHL17 (II)
AHL18(II)
AHL19(II)
AHL20(II)
AHL21(II)
AHL22(II)
AHL23(II)
AHL24(II)
AHL25(II)
AHL26(II)
AHL27(II)
AHL28(II)
AHL29(II)

Jiang_Fig S2

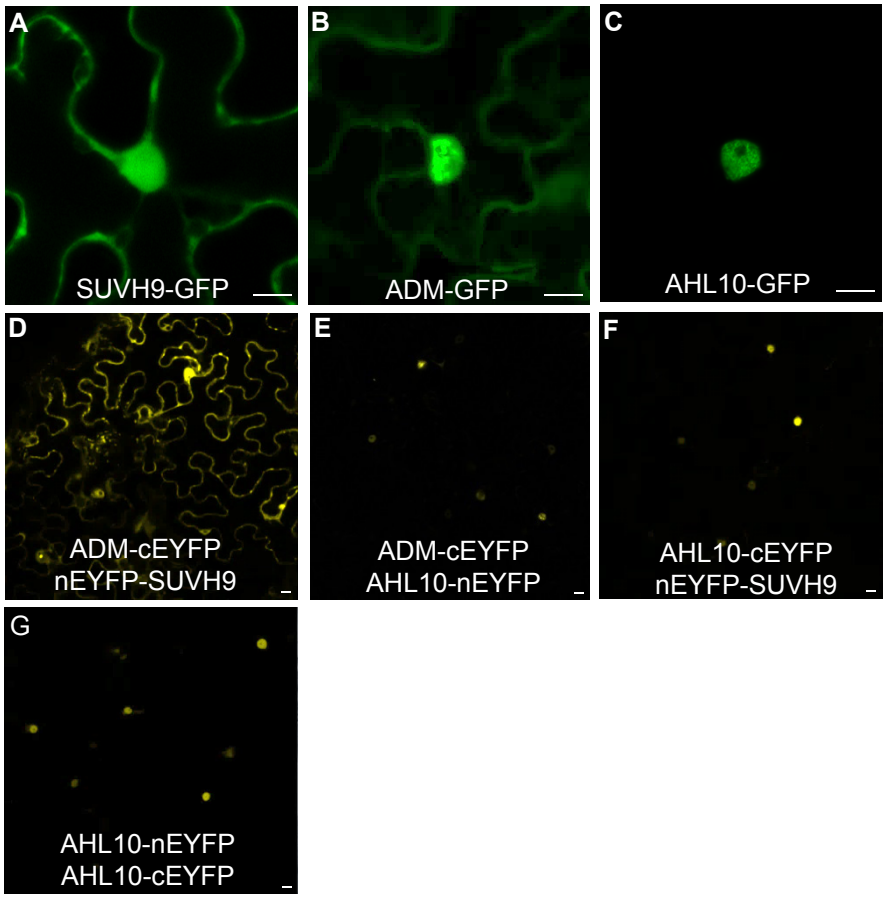
A
SUVH9-GFP
B
ADM-GFP
C
AHL10-GFP
D
ADM-cEYFP
nEYFP-SUVH9
E
ADM-cEYFP
AHL10-nEYFP
F
AHL10-cEYFP
nEYFP-SUVH9
G
AHL10-nEYFP
AHL10-cEYFP

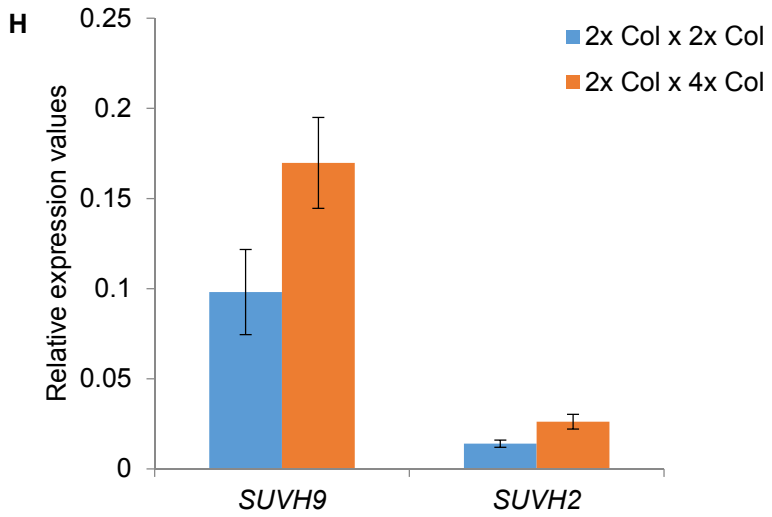
H
0.25
0.2
0.15
0.1
0.05
0
Relative expression values
2x Col x 2x Col
2x Col x 4x Col
SUVH9
SUVH2

Jiang_Fig S3

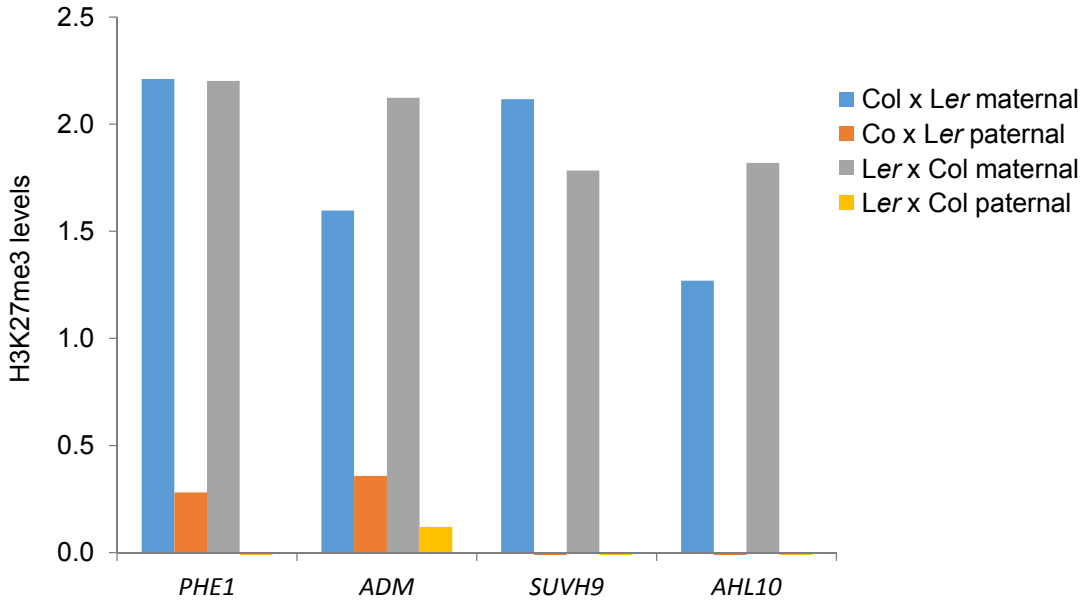
2.5
2.0
1.5
1.0
0.5
0.0
H3K27me3 levels
PHE1
ADM
SUVH9
AHL10
Col x Ler maternal
Co x Ler paternal
Ler x Col maternal
Ler x Col paternal

Jiang_Fig S4

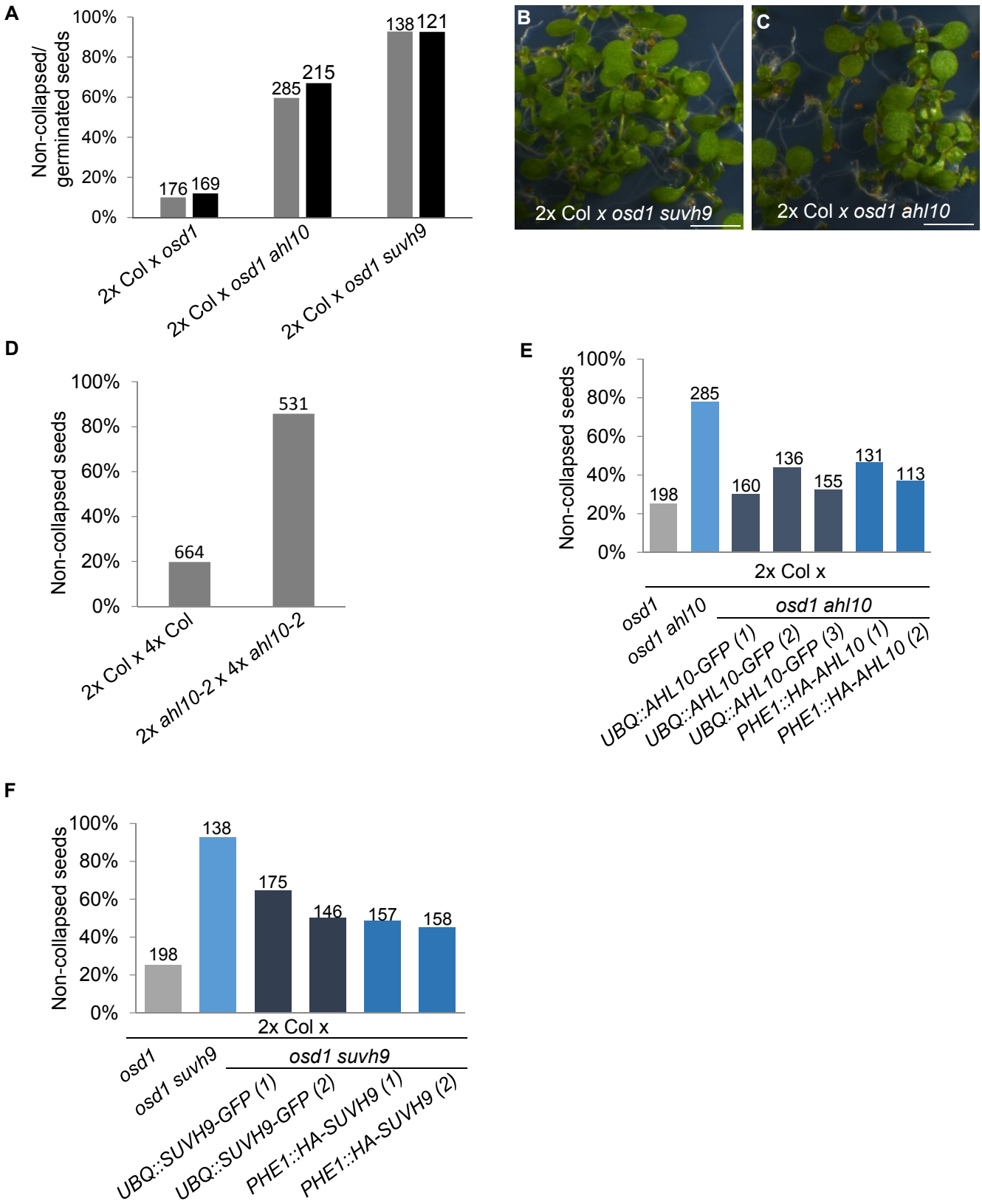
A
Non-collapsed/ germinated seeds
100%
80%
60%
40%
20%
0%
176
169
285
215
138
121
2x Col x osd1
2x Col x osd1 ahl10
2x Col x osd1 suvh9
B
2x Col x osd1 suvh9
C
2x Col x osd1 ahl10
D
Non-collapsed seeds
664
531
2x Col x 4x Col
2x ahl10-2 x 4x ahl10-2
E
Non-collapsed seeds
198
285
160
136
155
131
113
2x Col x
osd1
osd1 ahl10
osd1 ahl10
UBQ::AHL10-GFP (1)
UBQ::AHL10-GFP (2)
UBQ::AHL10-GFP (3)
PHE1::HA-AHL10 (1)
PHE1::HA-AHL10 (2)
F
Non-collapsed seeds
198
138
175
146
157
158
2x Col x
osd1
osd1 suvh9
osd1 suvh9
UBQ::SUVH9-GFP (1)
UBQ::SUVH9-GFP (2)
PHE1::HA-SUVH9 (1)
PHE1::HA-SUVH9 (2)

Jiang_Fig S5

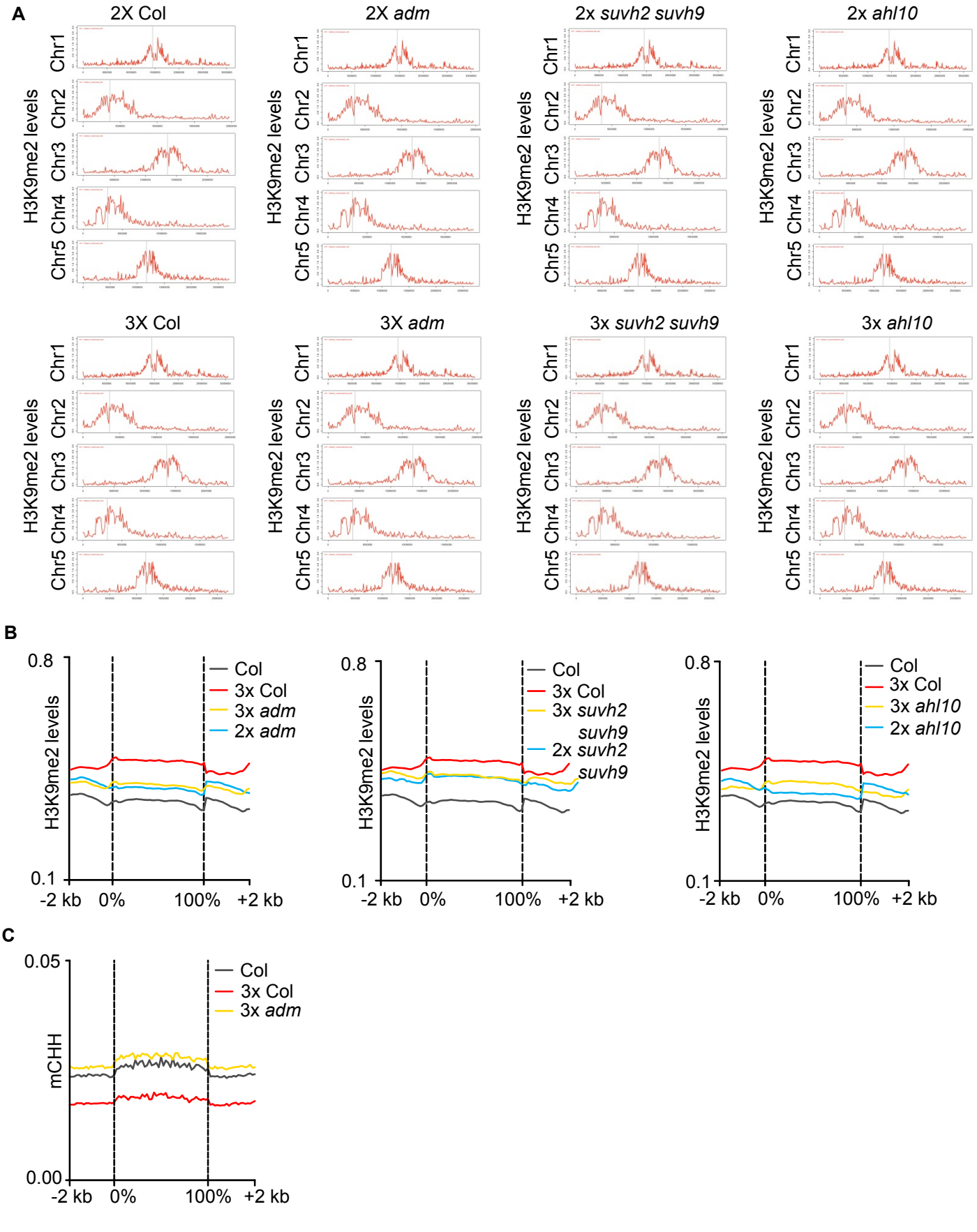
A
2X Col
2X adm
2x suvh2 suvh9
2x ahl10
3X Col
3X adm
3x suvh2 suvh9
3x ahl10
H3K9me2 levels
Chr1
Chr2
Chr3
Chr4
Chr5
B
0.8
0.1
H3K9me2 levels
Col
3x Col
3x adm
2x adm
3x suvh2 suvh9
2x suvh2 suvh9
3x ahl10
2x ahl10
-2 kb
0%
100%
+2 kb
C
0.05
0.00
mCHH

Jiang_Fig S6

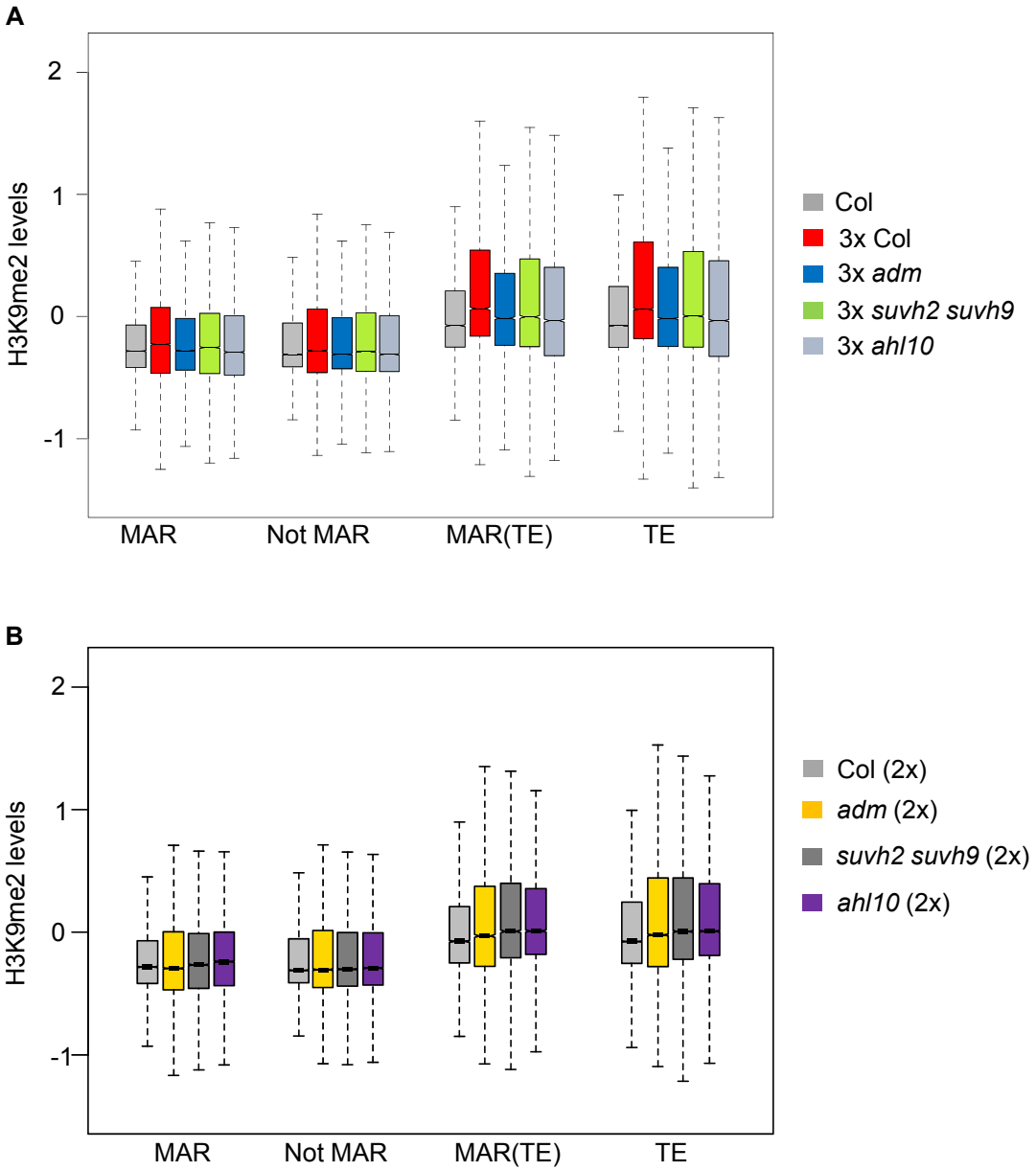
A
H3K9me2 levels
2
1
0
-1
MAR
Not MAR
MAR(TE)
TE
Col
3x Col
3x adm
3x suvh2 suvh9
3x ahl10
B
H3K9me2 levels
2
1
0
-1
MAR
Not MAR
MAR(TE)
TE
Col (2x)
adm (2x)
suvh2 suvh9 (2x)
ahl10 (2x)

Jiang_Fig S7

A

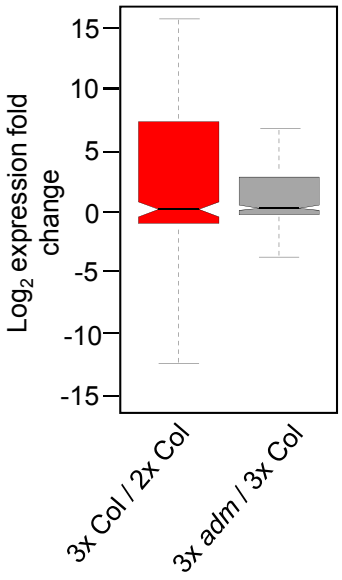

B

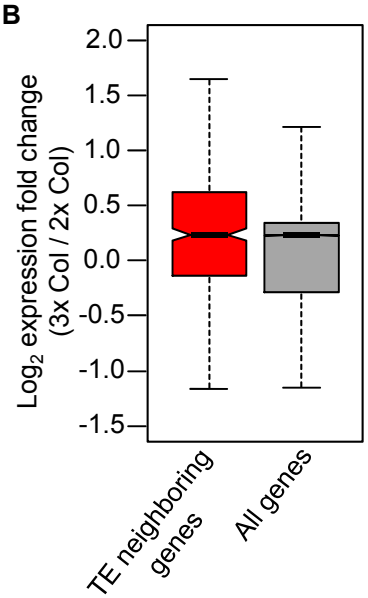

C

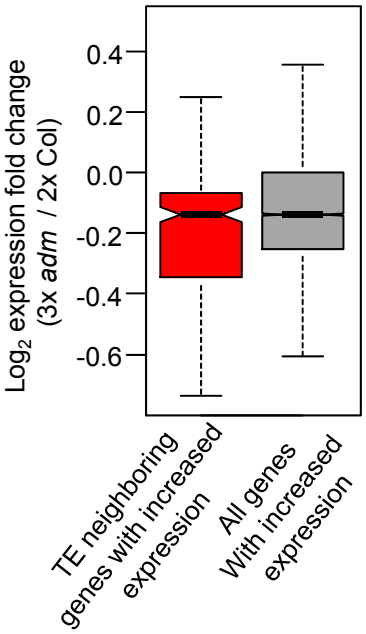

Jiang_Fig S8

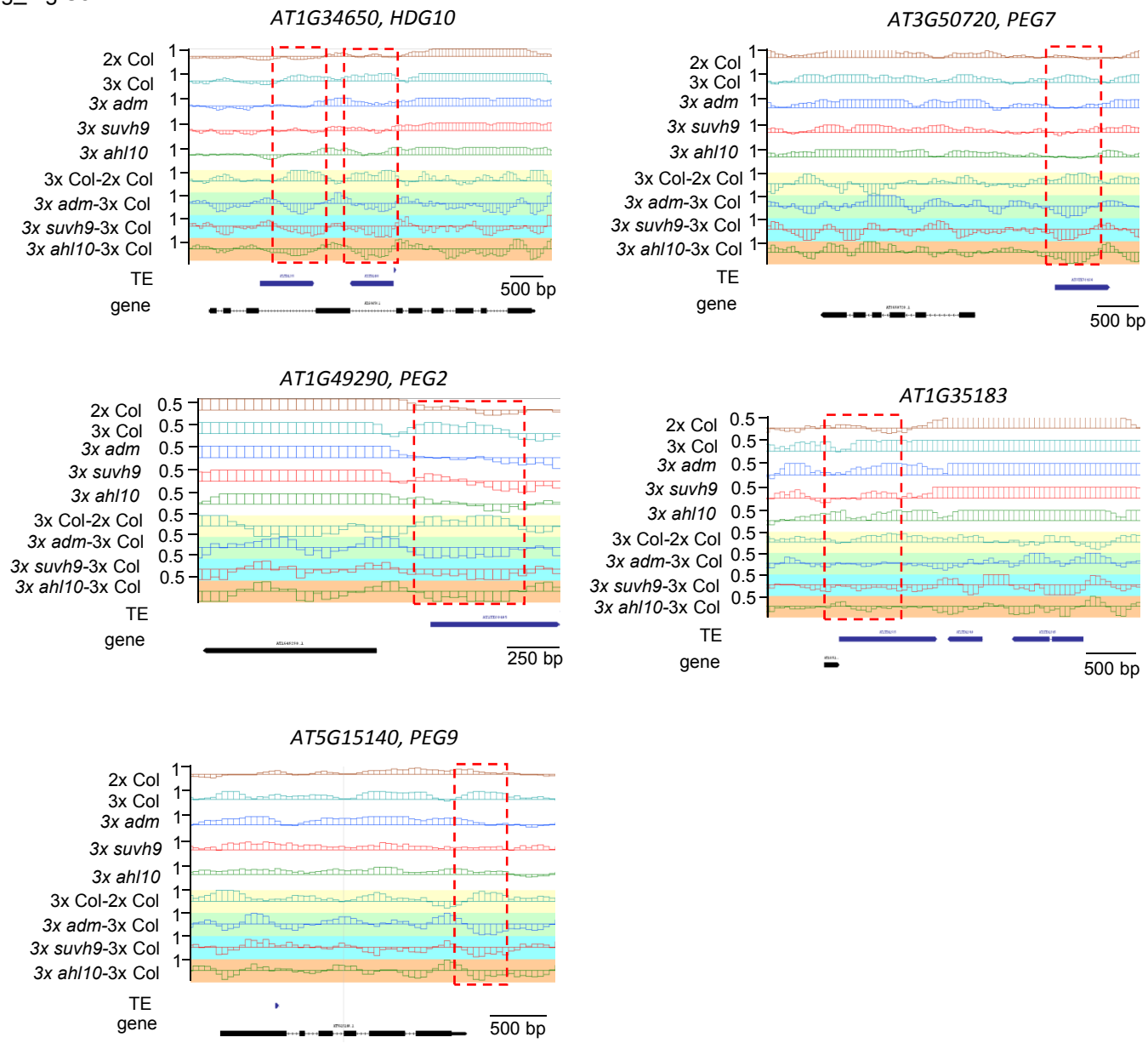
AT1G34650, HDG10
2x Col
3x Col
3x adm
3x suvh9
3x ahl10
3x Col-2x Col
3x adm-3x Col
3x suvh9-3x Col
3x ahl10-3x Col
TE
gene
500 bp
AT3G50720, PEG7
2x Col
3x Col
3x adm
3x suvh9
3x ahl10
3x Col-2x Col
3x adm-3x Col
3x suvh9-3x Col
3x ahl10-3x Col
TE
gene
500 bp
AT1G49290, PEG2
2x Col
3x Col
3x adm
3x suvh9
3x ahl10
3x Col-2x Col
3x adm-3x Col
3x suvh9-3x Col
3x ahl10-3x Col
TE
gene
250 bp
AT1G35183
2x Col
3x Col
3x adm
3x suvh9
3x ahl10
3x Col-2x Col
3x adm-3x Col
3x suvh9-3x Col
3x ahl10-3x Col
TE
gene
500 bp
AT5G15140, PEG9
2x Col
3x Col
3x adm
3x suvh9
3x ahl10
3x Col-2x Col
3x adm-3x Col
3x suvh9-3x Col
3x ahl10-3x Col
TE
gene
500 bp

Jiang_Fig S9

A

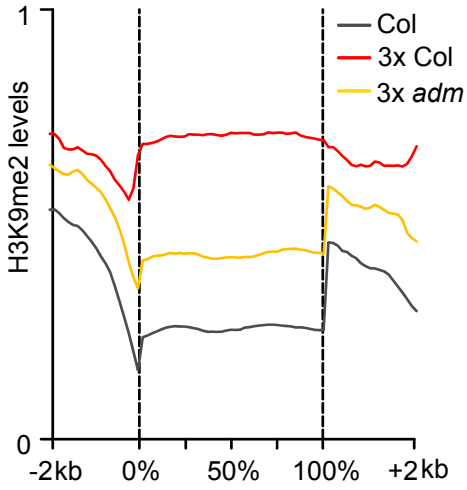

B

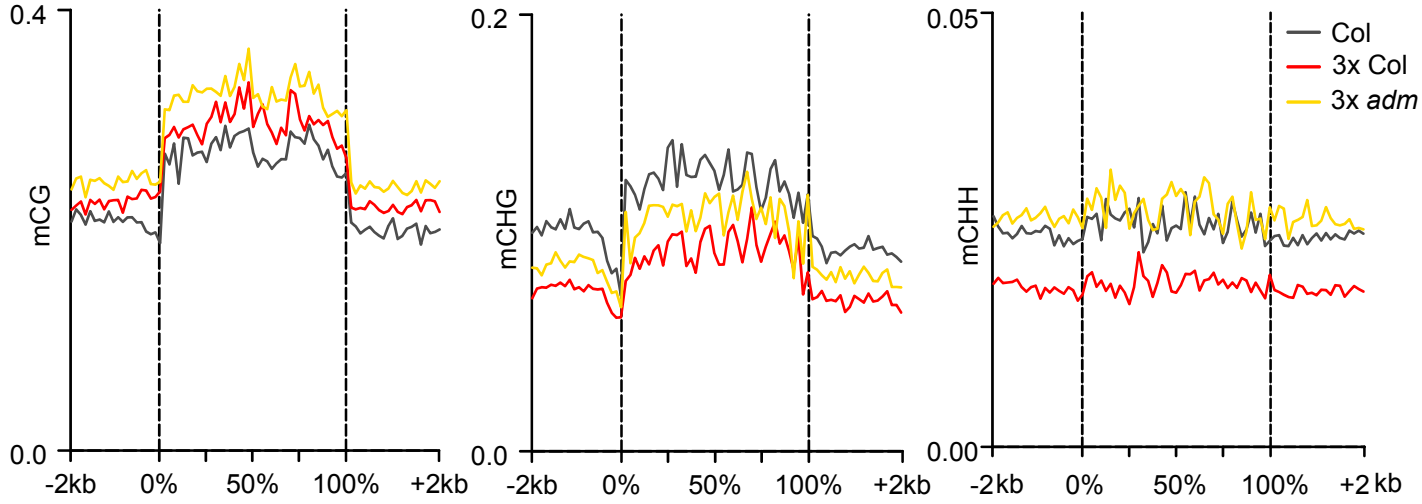

C

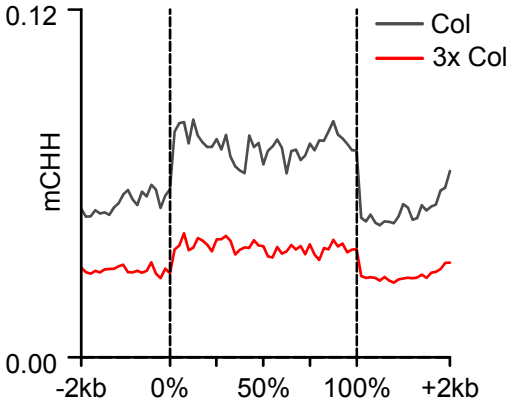

Jiang_Fig S10